Structural Engineering and Mechanics, *Vol. 74, No. 4 (2020) 547-557*
DOI: https://doi.org/10.12989/sem.2020.74.4.547

A new adaptive mesh refinement strategy based on a probabilistic error estimation

H. Ziaei and H. Moslemi*

Department of Civil Engineering, Shahed University, Persian Gulf Highway, Tehran, Iran

(Received April 2, 2019, Revised January 2, 2020, Accepted January 3, 2020)

Abstract. In this paper, an automatic adaptive mesh refinement procedure is presented for two-dimensional problems on the basis of a new probabilistic error estimator. First-order perturbation theory is employed to determine the lower and upper bounds of the structural displacements and stresses considering uncertainties in geometric sizes, material properties and loading conditions. A new probabilistic error estimator is proposed to reduce the mesh dependency of the responses dispersion. The suggested error estimator neglects the refinement at the critical points with stress concentration. Therefore, the proposed strategy is combined with the classic adaptive mesh refinement to achieve an optimal mesh refined properly in regions with either high gradients or high dispersion of the responses. Several numerical examples are illustrated to demonstrate the efficiency, accuracy and robustness of the proposed computational algorithm and the results are compared with the classic adaptive mesh refinement strategy described in the literature.

Keywords: adaptive mesh refinement; error estimation; stochastic finite element; mesh dependency; first-order perturbation theory

1. Introduction

Uncertainties in structural parameters and their effect on the response of the structure are continuously gaining in significance. These uncertainties may be resulted from manufacturing tolerances, determining external forces, insufficient data on material properties and imprecise statistical data. In the last three decades nondeterministic analysis of engineering structures has received considerable attention of an increasing number of researchers. Numerical techniques have become widely used methods to develop the field of stochastic mechanics in large and highly-complex problems with the help of the fast computing technology. Various techniques for discretization of the random fields in random variables are presented in the literature (Li and Der Kiureghian 1993). The stochastic finite element method is one of the powerful tools in computational stochastic mechanics. However, the mesh dependency of the simulation results remains a topic of concern. To overcome this drawback, several adaptive mesh refinement strategies have been proposed in the recent years.

One of the challenging problems in numerical solutions of differential equations governing physical phenomena is the estimation of discretizing errors and how far is it from the exact solution. In most of the problems, the exact solution is unknown, and several methods have been proposed to estimate the error and improve the accuracy of the results. Richardson (1910) was one of the pioneers who applied error estimation in finite difference method. The estimated error in any mesh depends on the size of the mesh and the error function degree, also, depends on the method of the solution (Zienkiewicz 2006). The priori error estimators are one of the first methods for error estimation which didn’t provide any information on the exact value of error, and they determined the rate of convergence of the solution qualitatively using the general form of the solution (Grätsch and Bathe 2005). In another attitude called posteriori error estimation, an initial hypothesis about the form of the solution is used for error estimation. This type of error estimation can be generally divided into two different categories; the residual based and the recovery based techniques. In the residual-based method proposed by Babuška and Reinboldt (1987), after the solution by finite element method, the results for boundary points were placed in the governing differential equation and the residuals were calculated in a patch of elements. Özakça (2003) compared error estimators based on residual methods and discussed their performance, reliability and convergence.

On the other hand, Zienkiewicz and Zhu (1987) proposed recovery-based error estimation which improves the finite element solution through a recovery procedure to obtain a more accurate representation of the variables. In this procedure, the error is approximated by the difference between the recovered solution and finite element solution. Various recovery procedures were proposed in the literature starting from the simplest form of averaging at each node to the superconvergent patch recovery technique. The superconvergent patch recovery (SPR) technique introduced by Zienkiewicz and Zhu (1992) for recovery of the gradient values. They improved the recovery process using the superconvergence behavior in the Gauss points of the regular isoparametric elements. A similar technique was proposed by Boroomand and Zienkiewicz (1997) which

*Corresponding author, Ph.D.
E-mail: h.moslemi@shahed.ac.ir

http://www.techno-press.com/journals/sem&subpage=7
ISSN: 1225-4568 (Print), 1598-6217 (Online)

does not need to identify super-convergent points particularly in element without superconvergent points. Ródenas *et al.* (2008) applied SPR technique for the XFEM framework using different recovery methods for singular and smooth stress fields. Moslemi and Khoei (2009,2010) proposed the weighted superconvergent patch recovery (WSPR) which estimates the error more efficient and realistic particularly in crack problems. The SPR technique is enhanced by Gonzalez-Estrada *et al.* (2013) to be applied in goal-oriented error estimation recovering both primal and dual solutions. Kumar *et al.* (2017) developed a posteriori error estimator in isogeometric analysis (IGA) based on B-splines and LR B-splines for an elliptic model problem. A statistical approach for error estimation in adaptive finite element method was presented by Moslemi and Tavakkoli (2018) using the statistical distribution of the stress values at Gauss points. They proposed the new error estimator as the difference between the actual distribution and the uniform distribution function.

The study of error estimation strategies to drive adaptive mesh refinement in stochastic analysis has recently received considerable attention. Deb *et al.* (2001) presented a framework for the construction of Galerkin approximations of elliptic boundary-value problems with stochastic input data and utilized a theory of a posteriori error estimation and corresponding adaptive approaches based on practical experience. A posteriori error estimation for the numerical solution of a stochastic variational problem arising in the context of parametric uncertainties was presented by Mathelin and Le Maıtre (2007). The error is approximated using the discrete solution of the primal stochastic problem and two discrete adjoint solutions on two imbricated spaces of the associated dual stochastic problem. An interval arithmetic-based finite element analysis was used by Lee *et al.* (2008) to estimate the uncertainties in structural analyses. They constructed tree graphs of uncertain data by numerical uncertainty combinations of structural parameters. They extend this method to to evaluate behavior uncertainties of structures without the application of probability theory (Lee *et al.* 2017). Eigel *et al.* (2014) developed an anisotropic residual-based a posteriori error estimator which contains bounds for both contributions to the overall error: the error due to gpc discretization and the error due to finite element discretization of the Galerkin projection onto finite generalized polynomial chaos (gpc) coefficients in the expansion. An adaptive refinement strategy is presented which allows steering the polynomial degree adaptation and the dimension adaptation in the stochastic Galerkin discretization, and, embedded in the gpc adaptation loop, also the Finite Element mesh refinement of the gpc coefficients in the physical domain. Guignard *et al.* (2016) used a perturbation approach to expand up the random solution to a certain order with respect to a parameter that controls the amount of randomness in the input and discretized by finite elements. They derived a priori and a posteriori error estimates of the error between the exact and approximate solution in various norms, including goal-oriented error estimation. The stochastic Galerkin finite element method was implemented by Bespalov and Rocchi (2018) for numerical solution of elliptic PDE problems with correlated random data. The algorithm employs a hierarchical a posteriori error estimation strategy which also provides effective estimates of the error reduction for enhanced approximations. These error reduction indicators are used in the algorithm to perform a balanced adaptive refinement of spatial and parametric components of Galerkin approximations.

The present paper deals with the development of a new adaptive mesh refinement strategy for two-dimensional problems based on the probabilistic error estimation . The lower and upper bounds of the structural parameters are estimated using first-order perturbation theory. Since these intervals are strongly mesh dependent, the mesh should be refined in regions with higher tolerance of the results. A new error estimator based on the probabilistic tolerance is proposed and is combined with the classic one to consider both the dispersion and high gradient of the results. The proposed algorithm can easily be implemented as a postprocessor in available finite element packages. The layout of the remainder sections of the paper is organized as follows; Section 2, reviews a posteriori error estimation based on the WSPR technique proposed by Moslemi and Khoei (2009). Next, in Section 3, a novel adaptive mesh refinement strategy is introduced based on the probabilistic error estimation. Several numerical results demonstrating the robustness and the efficiency of proposed algorithm are presented in Section 4. Finally, Section 5 is devoted to some concluding remarks.

2. Adaptive mesh refinement

In the adaptive mesh refinement, the main purpose is to create an optimal mesh minimizing the computational costs while limiting of discretization error in the finite element solution to an acceptable limit. However, the exact value of the stress field is not known for most of the problems. Thus, the error is approximated as the difference between the recovered values and those obtained directly from the finite element solution. The results are improved by smoothing the finite element solution over a patch using weighted superconvergent patch recovery technique (WSPR) proposed by Moslemi and Khoei (2009). The concept of superconvergence is that at some points the rate of convergence is higher than that in other points. The Gauss integration points are also the superconvergent points for the regular isoparametric elements (Zienkiewicz and Zhu 1992). In WSPR technique, a polynomial is fitted over the Gauss points of the element patch surrounding the target node. The improved stress can be obtained as a polynomial with unknown coefficients for each component of σ^*_i by

$$\sigma_i^* = \mathbf{Pa} = \left\langle 1 \quad x \quad y \quad \dots \quad y^n \right\rangle \left\langle a_0 \quad a_1 \quad a_2 \quad \dots \quad a_n \right\rangle \quad (1)$$

where $\mathbf{P}$ contains the polynomial base functions and $\mathbf{a}$ denotes the vector of unknowns. A common method for determination of the unknown vector $\mathbf{a}$ is to perform a least square fit to the finite element solutions in the patch for considered vertex node. In this process, the number of Gauss points in the patch should be taken as greater than the

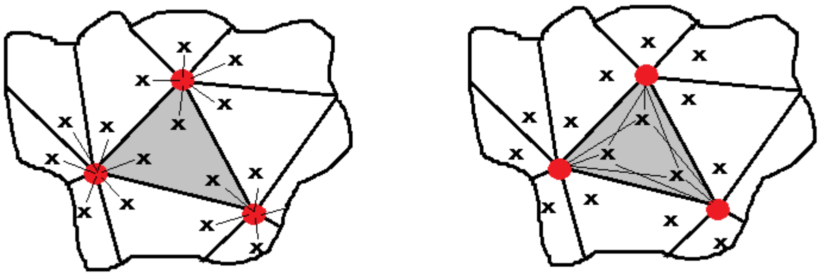

Fig. 1 The process of recovering of the stresses; ● nodal points, × Gauss points

number of unknown parameters in the polynomial. In the case of boundary nodes which have few Gauss points in the patch, the patch can be expanded to adjacent elements. In the WSPR technique different weighting parameters are assumed for the sampling points of the patch in the error functions. This results a more realistic recovered value of stress at the nodal point particularly in the boundary regions. The error function can be written as the difference between improved solution σ^* and finite element solution $\hat{\sigma}$, i.e. $e = \sigma^* - \hat{\sigma}$. Applying WSPR technique for recovering the stresses and performing a least square fit will give the error function as:

$$F(\mathbf{a}) = \sum_{k=1}^{n} \left(w_k \left[\sigma_i^*(x_k, y_k) - \hat{\sigma}_i(x_k, y_k) \right] \right)^2 = \sum_{k=1}^{n} \left(w_k \left[\mathbf{P}(x_k, y_k)\mathbf{a} - \hat{\sigma}_i(x_k, y_k) \right] \right)^2 \quad (2)$$

where n is the number of the sampling points and (x_k, y_k) denotes their coordinates. To make the nearest sampling points more effective in the recovery process, the weighting factor w_k is taken as the distance between the recovered nodal point and the sampling point. Thus, the weighting parameter is defined $w_k=1/r_k$, with r_k denoting the distance of each sampling point from the vertex node which is under recovery. The vector of unknowns $\mathbf{a}$ is obtained by minimization of the error function F($\mathbf{a}$).

$$\mathbf{a} = \left(\sum_{k=1}^{n} w_k^2 \mathbf{P}_k^{\mathbf{T}} \mathbf{P}_k \right)^{-1} \sum_{k=1}^{n} \left(w_k^2 \mathbf{P}_k^{\mathbf{T}} \hat{\sigma}_i(x_k, y_k) \right) \quad (3)$$

The recovery of the stresses from Gauss points to nodal points is accomplished for all of the nodes of the domain. Then the nodal stresses are transferred to Gauss points by standard shape function of the element.

$$\sigma_{Gauss}^* = \mathbf{N}.\sigma^* \quad (4)$$

The process of the recovery of the stresses is illustrated schematically in Fig. 1. The approximation of stress error can be therefore written as the difference between the recovered values and those given directly by the finite element.

$$e_\sigma \approx \sigma_{Gauss}^* - \hat{\sigma} \quad (5)$$

This is a pointwise definition of error and is used for local refinement. To determine the accuracy of the overall solution, the error estimator is changed to a global parameter using the norm of error. The L_2 norm is usually employed for globalizing the error and defined as

$$\|e\| = \left(\int_\Omega e^T e \, d\Omega \right)^2 = \left(\int_\Omega \left(\sigma_{Gauss}^* - \hat{\sigma} \right)^T \left(\sigma_{Gauss}^* - \hat{\sigma} \right) d\Omega \right)^2 \quad (6)$$

where e is the error vector over the domain Ω. This norm can be evaluated in each element domain to achieve each element contribution in the total error. The square of the total error norm can be obtained by using the sum square root of elements error norm.

$$\|e_\sigma\|^2 = \sum_{i=1}^{m} \|e_\sigma\|_i^2 \quad (7)$$

with i denoting an element contribution and m the total number of elements. The distribution of error norm at the elements of domain depends on the problem and the discretization scheme. This distribution indicates the portions with high gradient stress field need refinement and other parts with uniform stress field need coarsening elements. This strategy leads to an optimal mesh with uniform distribution of error norm across the domain. To make the domain error independent of the problem type, the L_2 norm is normalized to the state variable, such as the stress norm. After the mesh refinement, this relative error should be less than the target percentage error, i.e.

$$\eta = \frac{\|e_\sigma\|}{\|\hat{\sigma}\|} \le \eta_{aim} = \frac{\|e_\sigma\|_{aim}}{\|\hat{\sigma}\|} \quad (8)$$

with η_{aim} denoting the prescribed target percentage error. The rate of convergence of local error in the standard elements depends on the order of shape functions. Thus, the new size of the elements for reaching the aim error can be evaluated as:

$$(h_i)_{new} = \left[\frac{\left(\|e_\sigma\|_i \right)_{aim}}{\|e_\sigma\|_i} \right]^{1/p} (h_i)_{old} \quad (9)$$

where p is the order of shape function. This process will lead to an element density distribution exported to a mesh generator to produce a new mesh with desired element sizes. In the mesh generator proposed here, the nodal element size is needed for creating the new mesh. Thus, the nodal element size is obtained using a simple averaging method on the Gauss points data around each node. After indicating the size of elements, a mesh satisfying the requirements will be finally generated by an efficient mesh generator which allows the new mesh to be constructed according to a predetermined size. However, to prevent the mesh generation difficulties, the element size is limited by an upper and a lower bound. To attain the aim error, several adaptive mesh refinement steps may be needed. In this condition the new mesh is considered as the old one for next step of adaptive remeshing.

3. Probabilistic error estimation

The classic adaptive finite element method described in Section 2, would lead to mesh refinement in high gradient regions such as load points, crack tips, strain localization regions, etc. The uncertainties in the system parameters such as geometric sizes, material properties and loading conditions, would affect the response tolerances. In finite element method, discretization error would intensify this tolerance and affect the design purposes. A proper mesh in finite element method would reduce the mesh dependency of response tolerances. The mesh would be refined in regions with higher tolerance and vice versa. The lower and upper bounds of the nodal displacements and stresses have been achieved using first-order perturbation theory. This theory is efficient and accurate when the uncertainties are not too large. Let random vector $R = \{R_1, R_2, \ldots R_n\}$ represent all random variables of the structural system. In two dimensional linear systems, it may include elasticity module E, geometric sizes in two directions L_x, L_y, thickness t and load vector F. In the displacement based finite element method, the equilibrium equation can be written as

$$[K]\{u\} = \{F\} \tag{10}$$

where $[K]$ is the stochastic global stiffness matrix; $\{u\}$ is the nodal displacement vector and $\{F\}$ is the stochastic force vector. Stochastic stiffness matrix and force vector can be related to the mean value and random variables as

$$K(R) = \bar{K} + \sum_{i=1}^{n} \frac{\partial K}{\partial R_i} dR_i = \bar{K} + dK \tag{11}$$

$$F(R) = \bar{F} + \sum_{i=1}^{n} \frac{\partial F}{\partial R_i} dR_i = \bar{F} + dF \tag{12}$$

where $\bar{K}$ and $\bar{F}$ are mean values of stiffness matrix and force vector. The variation of force vector is a random variable. To express the variation of stiffness matrix dK in terms of random variables, the stiffness matrix in two dimensional problems is written as

$$[K] = \int_A B^T DB \ t.dA \tag{13}$$

where B, D, t denote the generalized gradient matrix, material property matrix and thickness of the problem, respectively and A is the domain area. Thus, the variation of stiffness matrix can be expressed as

$$dK = \int_A \begin{pmatrix} dB^T DB\, t + B^T dDB\, t \\ +B^T DdB\, t + B^T DB\, dt \end{pmatrix} dA \tag{14}$$

The generalized gradient matrix B can be obtained differentiation of shape functions as

$$B_i = \begin{bmatrix} \partial N_i/\partial x & 0 \\ 0 & \partial N_i/\partial y \\ \partial N_i/\partial y & \partial N_i/\partial x \end{bmatrix} \tag{15}$$

The variation of each component of this matrix is affected by the planar geometric random variables. For instance the variation of the first component of this matrix can be expressed as

$$dB_{11} = \sum_{i=1}^{m} \frac{\partial^2 N_1}{\partial x^2} x_i dL_x \tag{16}$$

where m is the number of nodes in each element, x_i denotes the coordinates of each node of the element and dL_x is the geometry size random variable in x direction. Substituting dK and dF in Eqs. 11,12 and applying them into Eq. 10 gives the tolerance of nodal displacement.

$$\begin{aligned} du &= d(K^{-1})F + K^{-1}dF \\ &= -K^{-1}.dK.K^{-1}F + K^{-1}dF \end{aligned} \tag{17}$$

This leads to the lower and upper bounds of the nodal displacements and determines the nodes with higher tolerance in displacements. Using root sum squared method the x , y components of nodal displacements are combined and then it is normalized with respect to the average domain displacement. This normalized tolerance is taken as the probabilistic error estimator in correspondence with the classic error estimator.

$$e_{pr} \approx \frac{\|du\|}{\|u\|} \tag{18}$$

After defining new probabilistic error estimator, the remaining stages of adaptive mesh refinement is similar to the classic method through Eqs. (6)-(9). This process results to a new element density distribution with finer mesh in regions with the higher tolerance of results and larger mesh in elements with more determinant results. It is evident that each of the classic and probabilistic mesh refinements only affect their correspondent parameters. To attain a mesh with the proper classic and probabilistic estimated error, these two mesh refinements are combined together. In this way, the optimal mesh would be refined properly in regions with either high gradients or high dispersion of the responses. The new size of the elements in the combinational case is defined as the geometrical mean of new sizes in classic and probabilistic adaptive mesh refinement.

$$\left(h_i\right)_{new,combinational} = \sqrt{\left(h_i\right)_{new,classic} \times \left(h_i\right)_{new,probabilistic}} \quad (19)$$

Although this combined form of mesh refinement, does not act as effective as each of classic and probabilistic methods individually, but it will reduce the estimated errors totally.

4. Numerical simulation results

To demonstrate the capability and efficiency of the proposed probabilistic error estimator described in section 3, some examples are analyzed numerically. Three different examples are investigated where the adaptive mesh refinement is accomplished using classic, probabilistic and combined error estimation. To challenge the ability of the algorithm, several different uncertainties are considered in the examples such as geometry size, material properties, crack length and impact load position. The uncertainty in material properties can be modeled as the variation in constitutive matrix as shown in Eq. 14. However, the uncertainties in geometric parameters such as size of the domain, crack length and position of the load can be considered via the variation of nodal coordinates, as described in Eq. 16. These coefficients of variation are input values of the model and may be obtained through the statistical analysis on the survey data. In the finite element analysis, the two dimensional triangular elements with the three Gauss quadrature points for the numerical integration are used. A coarse uniform FE mesh is taken for the initialization of the remeshing process in all of the examples. The proposed algorithm would identify automatically the parts of the domain which require finer mesh in each of the classic and probabilistic approaches. In simulation of the crack propagation in third example, the formulation of maximum circumferential stress criterion (Erdogan and Sih 1963) is employed to determine the crack growth direction. The tolerance of the results in the DOFs have been achieved using first-order perturbation theory. To investigate the effect of adaptive mesh refinement using the probabilistic error estimation, the estimated errors are compared for the uniform, classic and probabilistic adapted meshes.

4.1 A bi-material square plate with different coefficient of variation

The first example is of a bi-material square plate with different coefficient of variation subjected to two concentrated tensile loads, as shown in Fig. 2-a. The coefficient of variation of elasticity modulus is 5% for the right half and 1% for the left half of the plate. The coefficient of variation of geometry size for in plane and out

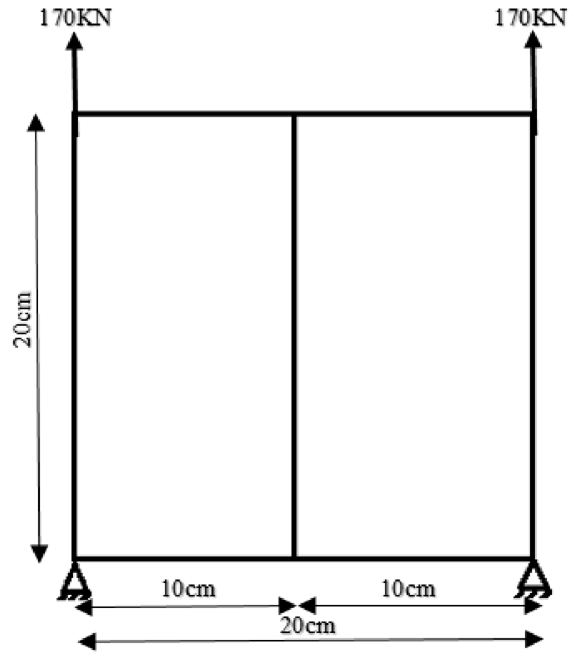

(a)

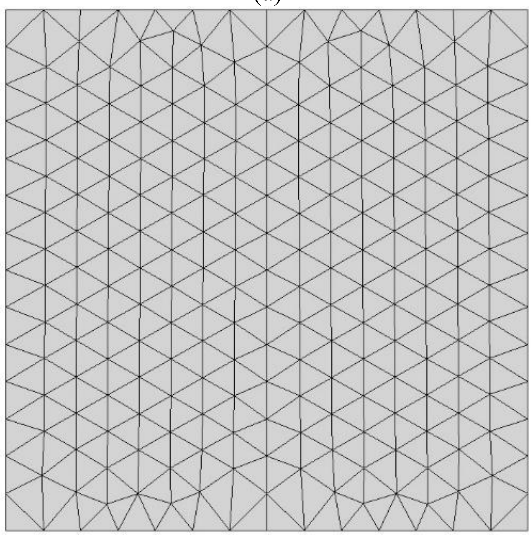

(b)

Fig. 2 The bi-material plate with different coefficient of variation; a) geometry and boundary conditions b) initial FE mesh

of plane dimensions is taken 1%. This example is chosen to compare the classic and probabilistic adaptive techniques for a benchmark problem. The initial coarse uniform mesh with 249 elements and 440 nodes.is shown in Fig 2-b.

The finite element analysis of the initial mesh illustrates the stress concentration at the concentrated loads and restrained points of the plate. Thus, the classic estimated error is locally high at these points regardless of different coefficient of variation. A very fine mesh refinement can be also observed at these regions as shown in Fig 3. This remeshing process have reduced the classic estimated error from 37.6% in initial mesh to 4.1% in the classic adaptive mesh. The probabilistic estimated error have also been reduced from 5.0% to 4.2% as shown in Table 1.

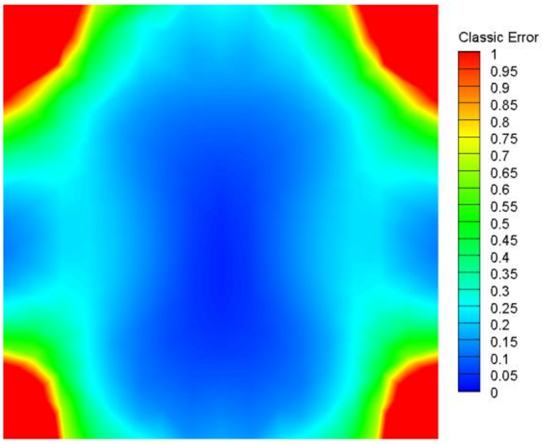

(a)

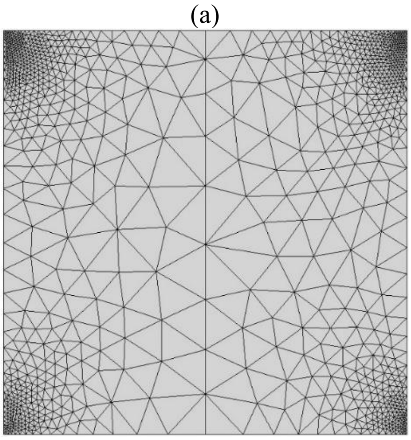

(b)

Fig. 3 The bi-material plate with different coefficient of variation; a) classic estimated error b) classic adaptive mesh

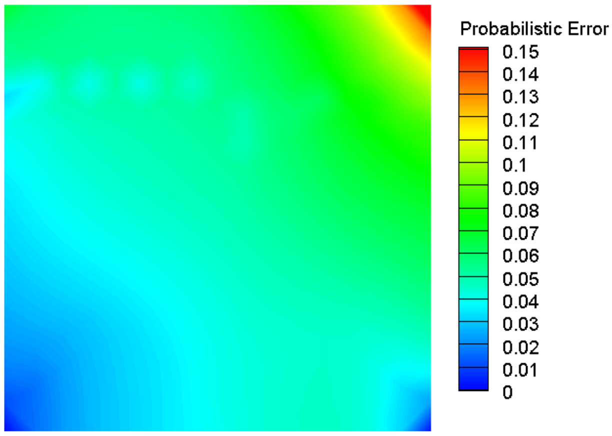

(a)

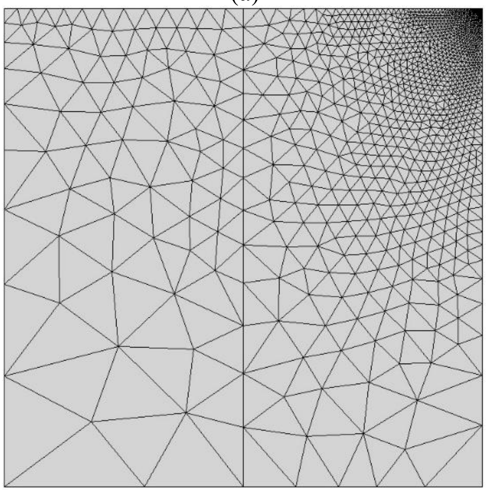

(b)

Fig. 4 The bi-material plate with different coefficient of variation; a) probabilistic estimated error b) probabilistic adaptive mesh

In next step, the error of the initial mesh is estimated according to the tolerance of the displacements as it was described in Section 3. The contour of estimated probabilistic error is shown in Fig. 4.a. Due to the higher coefficient of variation, the right half of the plate had a larger value of probabilistic error. It is evident that in restrained points the displacements are determinant and the probabilistic error is zero. Moving toward the top of the plate, the tolerance of the results would increase and the maximum probabilistic error occurs at the top right corner of the plate. The resultant adaptive mesh obtained in this approach is shown in Fig. 4.b. In this approach, the classic error is reduced from 37.6% in initial mesh to 7.4% in the probabilistic adaptive mesh. The probabilistic estimated error have also been reduced from 5.0% to 2.8% as shown in Table 1. It can be seen that this approach leads to more reduction of probabilistic error than the classic method.

Comparing these two approaches illustrates each approach is more successful in reduction of corresponding error value. Thus, an intermediate case is the combinational approach described in Section 3 where the new size of the elements can be obtained from Eq. 19. In this case the mesh is refined at stress concentration regions and in the right half of the plate with higher coefficient of variant, as shown in Fig. 5.a. The contours of the reduced classic error and probabilistic error for the combinational mesh are shown in Figs. 5.b and 5.c. The classic error have been reduced to 6.5% and the probabilistic error have been reduced to 3.3% in the combined approach. It indicates that this combined approach would result a balanced reduction in both error indices. The estimated error for different uniform and adapted meshes are summarized in Table 1.

4.2 Cracked beam with uncertainty on crack length

The second example is a bending beam with an 8 cm crack which is subjected to a midspan 300 kN concentrated load as shown in Fig. 6.a. The geometry, boundary condition and initial FE mesh with 205 nodes and 348 elements are indicated in Fig. 6. In this example, the coefficient of variation in geometry dimensions and elasticity modulus is taken 1% all over the domain. In addition the uncertainty in the initial crack length is taken 10%. This uncertainty affects the nodal coordinates of the FE mesh especially near the crack.

The classic finite element analysis indicates that the focus of estimated error is near the concentrated loads and

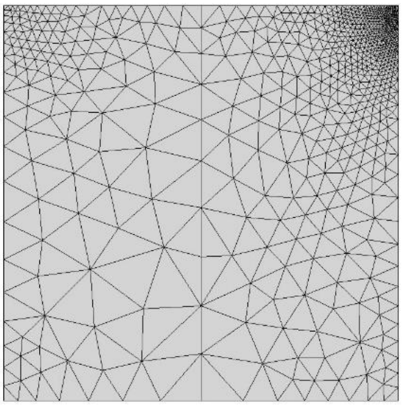

(a)

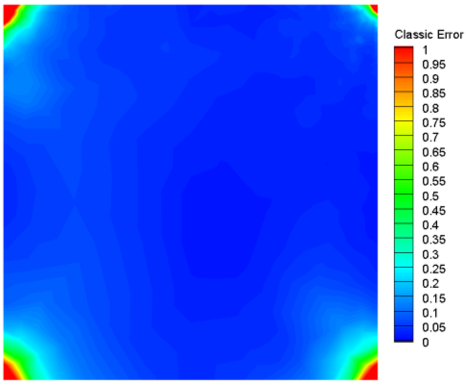

(b)

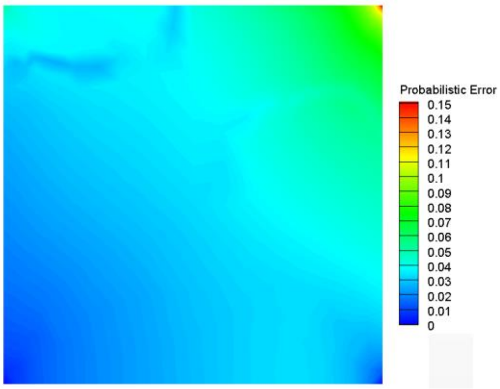

(c)

Fig. 5. The bi-material plate with different coefficient of variation; a) combinatioanl adaptive mesh, b) classic estimated error, c) probabilistic estimated error

Table 1 The bi-material plate with different coefficient of variation; Summary of estimated errors for different uniform and adapted meshes

parameters / mesh type	number of nodes	number of elements	estimated classic error	estimated probabilistic error
initial mesh	249	440	0.3765	0.05
classic adaptive mesh	1221	2280	0.0414	0.0419
probabilistic adaptive mesh	1223	2312	0.0739	0.0283
combinational adaptive mesh	845	1566	0.0650	0.0334

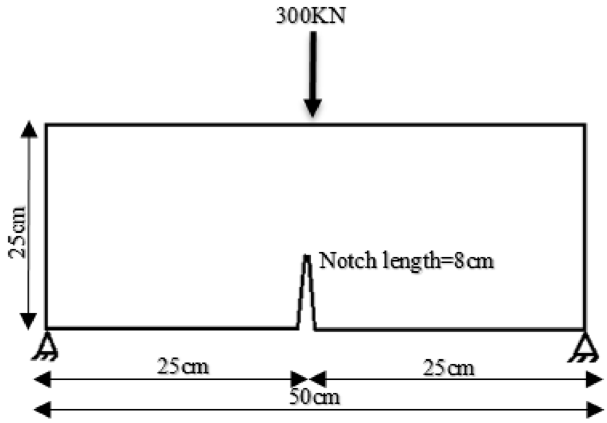

(a)

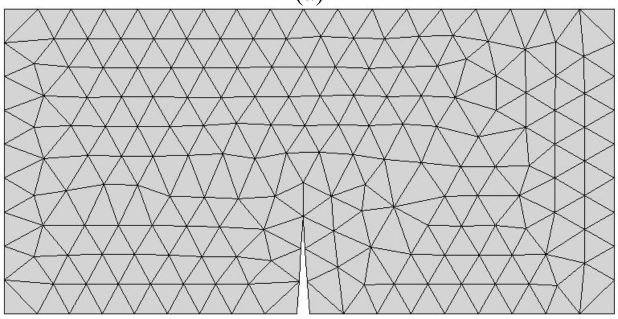

(b)

Fig. 6 Cracked beam with uncertainty on crack length; a)geometry and boundary conditions, b) initial FE mesh

restraints. Due to the singular stress field near the crack tip in linear elastic fracture mechanics (LEFM), the crack tip zone shows a high value of error. The contour of classic estimated error in Fig. 7.a confirms this behavior.

The classic adaptive mesh as shown in Fig. 7.b have applied the refinement near the load, restraints and near the crack tip zone which is in concordance with the contour of error. Table 2 shows that the classic estimated error have been reduced drastically from 36.9% in the initial mesh to 2.9% after adaptive mesh refinement, but the probabilistic estimated error is reduced slightly from 3.9% to 2.8%.

On the other hand, probabilistic adaptive mesh refinement accomplished on the initial mesh using proposed algorithm. The variation of crack length has led to a high probabilistic estimated error in a vertical band around the crack. This effect is more highlighted under the load (high tolerance in vertical displacement) and near the crack opening mouth (high tolerance in horizontal displacement). The distribution of the probabilistic error is shown in Fig. 8.a. To distribute the probabilistic error uniformly over the elements, the remeshing process is accomplished and the probabilistic adaptive mesh is obtained as shown in Fig. 8.b. Through this procedure the probabilistic error have reached to 2.4%. Due to the high uncertainties of the problem, the reduction of the probabilistic error is very limited.

To balance the reduction of classic and probabilistic error, the combinational adaptive mesh refinement is accomplished on the initial mesh. Since the region near the concentrated load experience high value of error in both of the approaches, very high dense mesh is generated in this

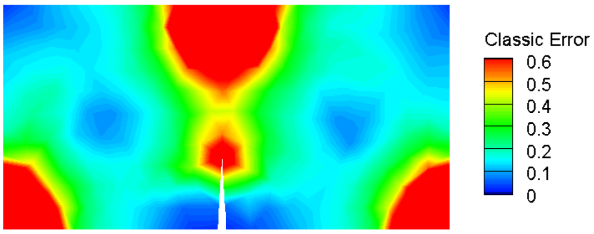

(a)

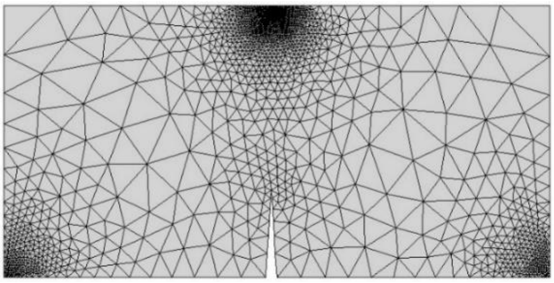

(b)

Fig. 7 Cracked beam with uncertainty on crack length; a) classic estimated error b) classic adaptive mesh

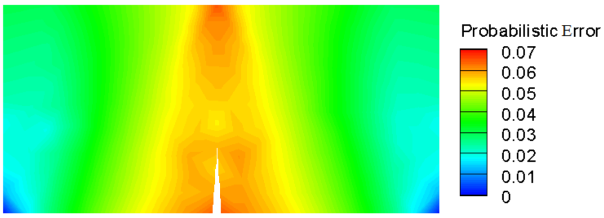

(a)

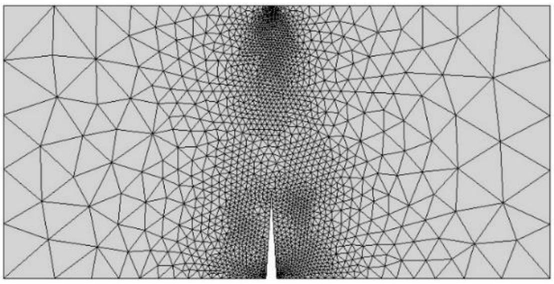

(b)

Fig. 8 Cracked beam with uncertainty on crack length; a) probabilistic estimated error b) probabilistic adaptive mesh

region using combinational. The concentrated restraints and vertical band near the crack have relative fine mesh and other parts of the domain are meshed with coarse elements algorithm as shown in Fig. 9.a. The effect of combinational adaptive mesh refinement is illustrated through contours of the reduced classic error and probabilistic error in Figs. 9.b and 9.c. The estimated error for different uniform and adapted meshes are summarized in Table 2. It can be seen from Table 2 that another advantage of combinational method is the balanced reduction of error with lower number of degrees of freedom (1205 nodes vs. 1950 nodes).

Table 2 Cracked beam with uncertainty on crack length; Summary of estimated errors for different uniform and adapted meshes

parameters / mesh type	number of nodes	number of elements	estimated classic error	estimated probabilistic error
initial mesh	205	348	0.3689	0.0385
classic adaptive mesh	1914	3685	0.0294	0.0283
probabilistic adaptive mesh	1950	3754	0.1146	0.0243
combinational adaptive mesh	1205	2305	0.0457	0.0246

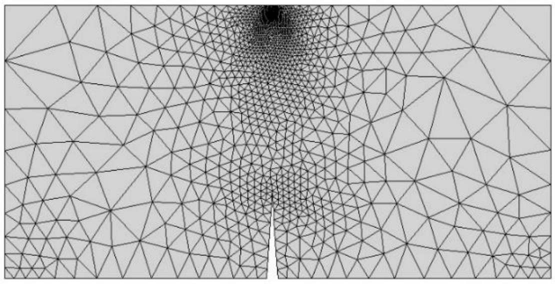

(a)

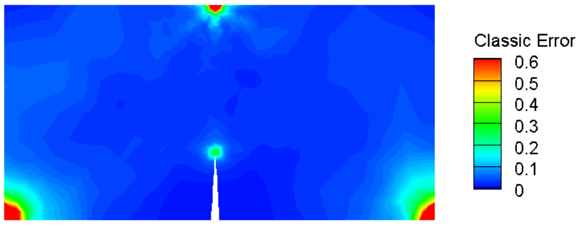

(b)

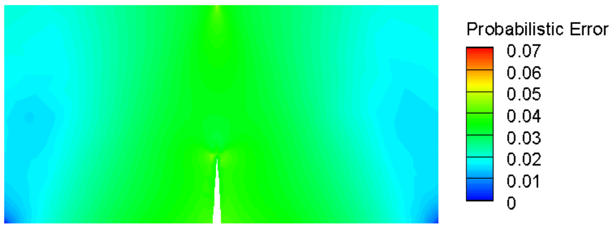

(c)

Fig. 9 Cracked beam with uncertainty on crack length; a) combinatioanl adaptive mesh, b) classic estimated error, c) probabilistic estimated error

4.3 Mixed mode crack growth with uncertainty on impact load position

The last example presents a simply supported beam with an edge notch at 13 cm from the center of beam. The eccentric crack leads to the mixed combination of mode I and II crack behavior. A 500 kN impact load is exerted to the center of top edge of the beam. The geometry and boundary conditions of the beam are shown in the Fig. 10.a. This example is chosen to demonstrate the effect of probabilistic mesh refinement on the upper bound and lower bound of crack growth trajectory. The beam is meshed initially with uniform coarse elements as shown in Fig. 10.b (205 nodes and 345 elements).

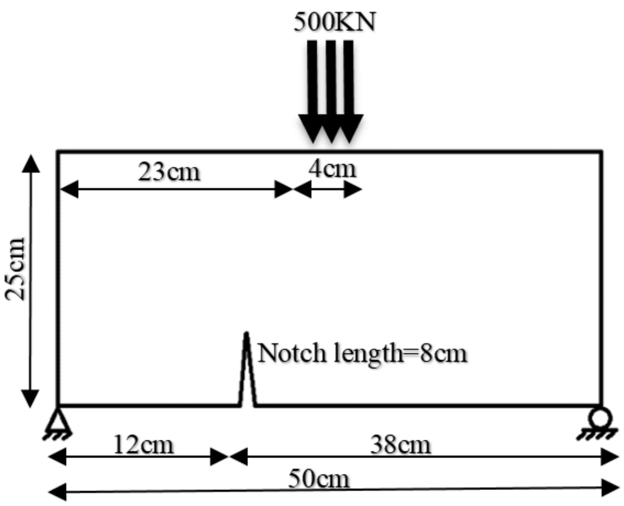

(a)

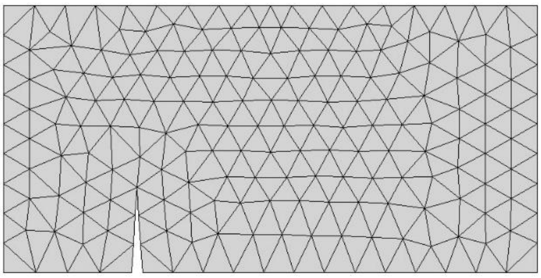

(b)

Fig. 10 Mixed mode crack growth with uncertainty on impact load position; a) geometry and boundary conditions, b) initial FE mesh

As with the previous example, the coefficient of variation in geometry dimensions and elasticity modulus is taken 1% all over the domain. In addition the uncertainty in the impact load position is taken 5%. The formulation of maximum circumferential stress criterion (Erdogan and Sih 1963) is employed to determine the crack growth direction. In this method, the stress components are recovered at the crack tip node, as described in Section 3. Based on this theory, the hoop stress reaches its maximum value on the plane of zero shear stress. The crack propagation angle θ can be expressed by using the angle between the line of crack and the crack growth direction.

$$\theta = \frac{1}{2}\ arctan\left(\frac{2\tau_{xy}}{\sigma_x - \sigma_y}\right) \tag{20}$$

where σ_x , σ_y , τ_{xy} are recovered stresses at the crack tip node and the positive value of θ defined in the anti-clockwise direction. The mixed mode behavior of the crack would turn the crack toward the midspan of the beam. Due to the uncertainty of the impact load position, the crack growth trajectory lies between an upper bound and lower bound. Since the discretization error would intensify the tolerance of uncertainties, analyzing the model with initial mesh would lead to a wide bound for the crack path. Applying the probabilistic adaptive mesh refinement, would narrow this bound. The contour of the probabilistic estimated error and its corresponding refined mesh is shown in Fig. 11.

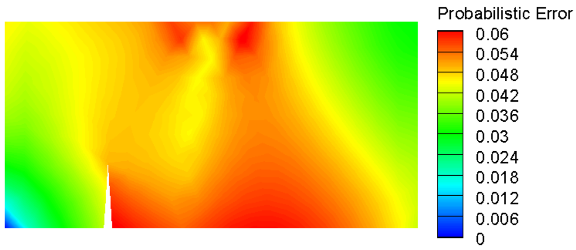

(a)

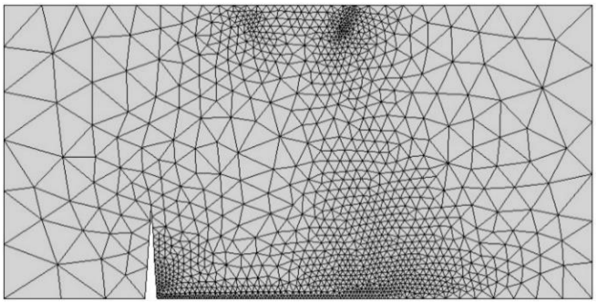

(b)

Fig. 11 Mixed mode crack growth with uncertainty on impact load position; a) probabilistic estimated error b) probabilistic adaptive mesh

The crack opening mouth sustains larger values of error especially on the left side of the beam where roller support generates higher tolerances in displacements. The bounds of the crack growth path have been calculated again according to the new adaptive mesh. Fig. 12 compares the bounds of the crack path obtained from initial mesh and probabilistic adaptive mesh. It is evident that the latter reduces the discretization error effect on displacement tolerances and lead to a narrower bound for crack growth path with more reliability. Like the previous examples, classic adaptive mesh refinement and combinational approach are also applied to this problem and the results are summarized in Table 3. It is obvious that the applying the proposed adaptive algorithms have reduced both of the classic and probabilistic estimated errors considerably. Combinational case shows a moderate and balanced reduction in both of error indices.

The crack opening mouth sustains larger values of error especially on the left side of the beam where roller support generates higher tolerances in displacements. The bounds of the crack growth path have been calculated again according to the new adaptive mesh. Fig. 12 compares the bounds of the crack path obtained from initial mesh and probabilistic adaptive mesh. It is evident that the latter reduces the discretization error effect on displacement tolerances and lead to a narrower bound for crack growth path with more reliability. Like the previous examples, classic adaptive mesh refinement and combinational approach are also applied to this problem and the results are summarized in Table 3. It is obvious that the applying the proposed adaptive algorithms have reduced both of the classic and probabilistic estimated errors considerably. Combinational

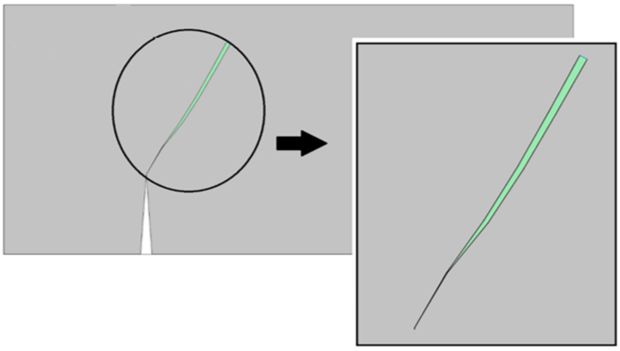

(a)

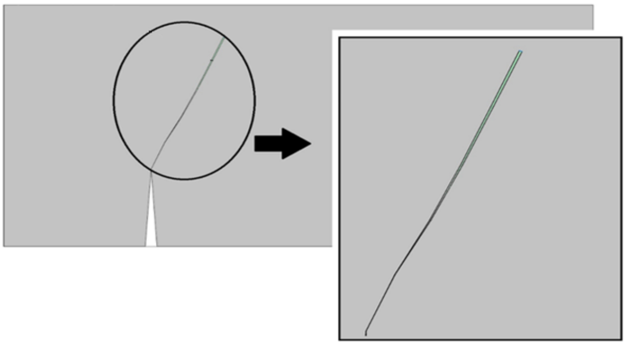

(b)

Fig. 12 Mixed mode crack growth with uncertainty on impact load position; a) the crack growth bounds with initial mesh b) the crack growth bounds with probabilistic adaptive mesh

Table 3 Mixed mode crack growth with uncertainty on impact load position; Summary of estimated errors for different uniform and adapted meshes

parameters / mesh type	number of nodes	number of elements	estimated classic error	estimated probabilistic error
initial mesh	226	376	0.4151	0.0794
classic adaptive mesh	1492	2835	0.0447	0.0399
probabilistic adaptive mesh	1503	2820	0.1313	0.0138
combinational adaptive mesh	1222	2283	0.0666	0.0199

case shows a moderate and balanced reduction in both of error indices.

5. Conclusion

In the present paper, a new probabilistic error estimator was presented for the reduction of mesh dependency in the tolerances of the FE results. The classic error estimators focus on the error reduction of the regions with high gradient stress field. However, in the stochastic problems high dispersion of the results would affect the design purposes. To reduce the discretization error in tolerance of the results, a new probabilistic error estimator was introduced based on first-order perturbation theory. The adaptive mesh in correspondence with error estimator refines the mesh in regions with higher tolerance of the results. The suggested error estimator neglects the refinement at the critical points with stress concentration. Therefore, the proposed strategy is combined with the classic adaptive mesh refinement to achieve an optimal mesh refined properly in regions with either high gradients or high dispersion of the responses. The efficiency and robustness of proposed adaptive algorithm in error reduction were presented by three numerical examples with different stochastic variables. The results indicated that each of the classic and probabilistic strategies have reduced corresponding error estimator considerably, but they have affected the other index moderately. The combinational strategy would result a balanced reduction in both error indices with lower number of degrees of freedom.

References

Babuška, I. and Rheinboldt, C. (1987), "A-posteriori error estimates for the finite element method", *Int. J. Numer. Methods Engrg*., **12**, 1597-1615. https://doi.org/10.1002/nme.1620121010.

Bespalov, A. and Rocchi, L. (2018), "Efficient adaptive algorithms for elliptic PDEs with random data", *SIAM/ASA J. Uncertain. Quantif.,* **6**, 243-272. https://doi.org/10.1137/17M1139928.

Boroomand. B. and Zienkiewicz, O.C. (1997), "Recovery by equilibrium: In patches (REP)", *J. Num. Meth. Eng*., **40**, 137-164. https://doi.org/10.1002/(SICI)1097-0207(19970115)40:1%3C137::AID-NME57%3E3.0.CO;2-5.

Deb, M.K., Babuška, I.M. and Oden, J.T. (2001), "Solution of stochastic partial differential equations using Galerkin finite element techniques", *Comput. Methods Appl. Mech. Eng,*. **190**, 6359-6372. https://doi.org/10.1016/S0045-7825(01)00237-7.

Eigel, M., Gittelson, C.J., Schwab, C. and Zander, E. (2014), "Adaptive stochastic Galerkin FEM", *Comput. Methods Appl. Mech. Eng*., **270**, 247-269. https://doi.org/10.1016/j.cma.2013.11.015.

Erdogan, F. and Sih G.C. (1963), "On the extension of plates under plane loading and transverse shear", *J. Basic Engng*., **4**, 519-527. https://doi.org/10.1115/1.3656897.

González-Estrada O.A., Nadal E., Ródenas J.J., Kerfriden P., Bordas S.P.A. and Fuenmayor F.J. (2013), "Mesh adaptivity driven by goal-oriented locally equilibrated superconvergent patch recovery", *Comput. Mech*., **53**, 957–976. https://doi.org/10.1007/s00466-013-0942-8.

Grätsch, T. and Bathe, K.J. (2005), "A posteriori error estimation techniques in practical finite element analysis", *Comput. Struct*., **83**, 235-265. https://doi.org/10.1016/j.compstruc.2004.08.011.

Guignard, D., Nobile, F. and Picasso, M. (2016), "A posteriori error estimation for elliptic partial differential equations with small uncertainties", *Numer. Methods Partial Differential Equations*, **32**, 175–212. https://doi.org/10.1002/num.21991.

Kumar, M., Kvamsdal, T. and Johannessen, K.A. (2017), "Superconvergent patch recovery and a posteriori error estimation technique in adaptive isogeometric analysis", *Comput. Methods Appl. Mech. Eng*., **316**, 1086–1156. https://doi.org/10.1016/j.cma.2016.11.014.

Lee, D.K., Park, S.S. and Shin, S.M. (2008), "Non-stochastic interval arithmetic-based finite element analysis for structural uncertainty response estimate", *Struct. Eng. Mech*., **29**, 469-488. https://doi.org/10.12989/sem.2008.29.5.469.

Lee, D.K and Shin, S.M. (2008), "Non-stochastic interval factor method-based FEA for structural stress responses with uncertainty", *Struct. Eng. Mech*., **62**, 703-708. https://doi.org/10.12989/sem.2017.62.6.703.

Li, C.C. and Der Kiureghian, A. (1993), “Optimal discretization of random fields”, *J. Engrg. Mech.*, **119**(6) 1136–1154. https://doi.org/10.1061/(ASCE)0733-9399(1993)119:6(1136).

Mathelin, L. and Le Maıtre, O. (2007), “Dual-based a posteriori error estimate for stochastic finite element methods”, *Commun. Appl. Math. Comput. Sci.*, **2**, 83–115. http://dx.doi.org/10.2140/camcos.2007.2.83.

Moslemi, H. and Khoei, A.R. (2009), “3D adaptive finite element modeling of non-planar curved crack growth using the weighted superconvergent patch recovery method”, *Eng. Fracture Mech.*, **76**, 1703–1728. https://doi.org/10.1016/j.engfracmech.2009.03.013.

Moslemi, H. and Khoei, A.R. (2010), “3D Modeling of damage growth and crack initiation using adaptive finite element technique”, *Scientia Iranica*, **17**, 372–386.

Moslemi, H. and Tavakkoli A. (2018), “A Statistical Approach for Error Estimation In Adaptive Finite Element Method”, *J. Comput. Methods Eng. Sci. Mech.*, **19**, 440-450. https://doi.org/10.1080/15502287.2018.1558424.

Özakça, M. (2003), “Comparison of error estimation methods and adaptivity for plane stress/strain problems”, *Struct. Eng. Mech.*, **15**, 579-608.

Richardson, L. (1910), “The approximate arithmetical solution by finite differences of physical problems”, *Transactions Royal Soc. London*, **210**, 307-357. https://doi.org/10.1098/rsta.1911.0009.

Ródenas, J.J., González-Estrada, O.A., Tarancón, J.E. and Fuenmayor, F.J. (2008), “A recovery-type error estimator for the extended finite element method based on singular+smooth stress field splitting”, *J. Numerical Methods Eng.*, **76**, 545–571. https://doi.org/10.1002/nme.2313.

Zienkiewicz, O.C. (2006), “The background of error estimation and adaptivity in finite element computation”, *Comput. Methods Appl. Mech. Eng.*, **195**, 207–213. https://doi.org/10.1016/j.cma.2004.07.053.

Zienkiewicz, O.C. and Zhu, J.Z. (1987), “A simple error estimator and adaptive procedure for practical engineering analysis”, *J. Num. Meth. Eng.*, **24**, 337-357. https://doi.org/10.1002/nme.1620240206.

Zienkiewicz, O.C. and Zhu, J.Z. (1992), “The super convergent patch recovery (SPR) and adaptive finite element refinement”, *Comp. Meth. Appl. Mech. Eng.*, **101**, 207-224. https://doi.org/10.1016/0045-7825(92)90023-D.

PL